Tissue injury and hypoxia promote malignant progression of prostate cancer by inducing CXCL13 expression in tumor myofibroblasts

Massimo Ammirante[a,b], Shabnam Shalapour[a,b], Youngjin Kang[a,b], Christina A. M. Jamieson[b], and Michael Karin[a,b,1]

[a]Laboratory of Gene Regulation and Signal Transduction, Department of Pharmacology and Pathology, and [b]Moores Cancer Center, School of Medicine, University of California, San Diego, La Jolla, CA, 92093

Prostate cancer (PC) is a slowly progressing malignancy that often responds to androgen ablation or chemotherapy by becoming more aggressive, acquiring a neuroendocrine phenotype, and undergoing metastatic spread. We found that B lymphocytes recruited into regressing androgen-deprived tumors by C-X-C motif chemokine 13 (CXCL13), a chemokine whose expression correlates with clinical severity, play an important role in malignant progression and metastatic dissemination of PC. We now describe how androgen ablation induces CXCL13 expression. In both allografted and spontaneous mouse PC, CXCL13 is expressed by tumor-associated myofibroblasts that are activated on androgen ablation through a hypoxia-dependent mechanism. The same cells produce CXCL13 after chemotherapy. Myofibroblast activation and CXCL13 expression also occur in the normal prostate after androgen deprivation, and CXCL13 is expressed by myofibroblasts in human PC. Hypoxia activates hypoxia-inducible factor 1 (HIF-1) and induces autocrine TGF-β signaling that promotes myofibroblast activation and CXCL13 induction. In addition to TGF-β receptor kinase inhibitors, myofibroblast activation and CXCL13 induction are blocked by phosphodiesterase 5 (PDE5) inhibitors. Both inhibitor types and myofibroblast immunodepletion block the emergence of castration-resistant PC in the transgenic adenocarcinoma of the mouse prostate (TRAMP) model of spontaneous metastatic PC with neuroendocrine differentiation.

tumor microenvironment | inflammation | cancer | cancer-associated fibroblasts

Prostate cancer (PC) is the most common nonskin malignancy among men and is a major cause of cancer-related death (1). Androgens, which support prostate growth and survival, are key factors in PC pathogenesis, and androgen ablation therapy is a well-established treatment strategy for hormone-dependent PC. However, in many cases, especially after androgen deprivation as well as chemotherapy or radiotherapy, PC progresses to an aggressive androgen-independent state known as castration-resistant PC (CRPC) that commonly metastasizes to bone and represents the major cause of PC mortality (1). CRPC development could also be a result of the emergence of neuroendocrine PC because of therapeutic intervention (2). Although neuroendocrine differentiation is rare in early PC, most drug-resistant and aggressive forms of PC exhibit a neuroendocrine phenotype (3–5). Treatment options for CRPC are limited, mostly because of intrinsic chemoresistance and the increased metastatic potential acquired by PC cells during disease progression (6). Identifying new targets for the prevention or treatment of CRPC and drug-resistant neuroendocrine PC is therefore of great importance.

The response to androgen withdrawal therapy is similar to any other treatment that triggers cell death and hypoxia (eg, chemotherapy), and this makes the CRPC system a general model for studying mechanisms underlying therapy-accelerated malignant progression, including neuroendocrine differentiation (2). We found that in addition to well-documented alterations in androgen receptor expression and signaling (7), CRPC development, at least in mice, is accelerated by inflammatory processes that are mediated by B

lymphocytes that are recruited into androgen-deprived PC by the chemoattractant C-X-C motif chemokine 13 (CXCL13) (8). We also described the presence of B lymphocytes in human PC, especially in more advanced disease (9). These PC-infiltrating lymphocytes produce cytokines, including lymphotoxin (LT), which leads to the activation of inhibitor of κB (IκB) kinase α (IKKα) within androgen-deprived PC cells, and thereby promote the survival and proliferation of CRPC-initiating cells (8). B lymphocytes producing LT may also be involved in metastatic progression (10).

In addition to innate and adaptive immune cells, the tumor microenvironment contains cancer-associated fibroblasts (CAFs), a heterogeneous population that plays important enabling roles in cancer development and progression (11–14). CAFs, which include normal tissue fibroblasts adjacent to the tumor as well as activated myofibroblasts, influence and modulate many properties of the evolving and progressing neoplasm through the secretion of extracellular matrix, matrix-modifying enzymes, growth factors, and cytokines. Via such mediators, as well as cell–cell contacts, CAFs exert growth-augmenting and survival effects on the malignant cell and thereby promote tumor angiogenesis and confer invasive and metastatic behaviors (12). CAFs produce inflammatory mediators through which they recruit immune cells into the tumor microenvironment and lead to their activation (15, 16). The exact origin of CAFs is a matter of active research, and they are thought to be derived either from tumor-proximal tissue fibroblasts or from local or bone marrow-derived mesenchymal stem cells (14, 17, 18). Among different

Significance

Prostate cancer often responds to hormone ablation therapy or chemotherapy by becoming more aggressive and metastatic. B cells recruited into hormone-deprived tumors by C-X-C motif chemokine 13 (CXCL13) play an important role in this process. We investigated how androgen ablation induces CXCL13 expression and found that CXCL13 is expressed by myofibroblasts within the tumor microenvironment that become activated as a result of low oxygen tension and hypoxia in androgen-deprived tumors. Hypoxia activates hypoxia-inducible factor 1 (HIF-1) and induces TGF-β expression, which converts fibroblasts to myofibroblasts and stimulates CXCL13 production. We show that several treatments that block CXCL13 expression, including immunodepletion of myofibroblasts, blockade of TGF-β signaling, and phosphodiesterase-5 (PDE5) inhibitors, inhibit B-cell recruitment into androgen-deprived prostate tumors and prevent the emergence of a more aggressive type of cancer.

CAF populations, myofibroblasts are characterized by the expression of α-smooth muscle actin (SMA) and fibroblast activation protein (FAP) and are normally derived from resident tissue fibroblasts on tissue injury and inflammation (18). Transient fibroblast proliferation and conversion to myofibroblasts are important for wound healing, but their persistent activation can lead to fibrosis (19). The mechanisms responsible for myofibroblast activation within the tumor microenvironment are not entirely clear and can be cancer-specific and heterogeneous. It is important to distinguish myofibroblasts, which are the descendants of proliferative fibroblasts (20, 21), from senescent fibroblasts, which do not proliferate but can produce a number of chemokines and cytokines, collectively known as the senescence secretory response (22). A recent study has shown that genotoxic cancer therapy induces CAF-mediated senescence secretory response in prostate tumors, a response that promotes resistance to chemotherapy (23).

We investigated the cell type responsible for expression of the B-cell chemoattractant CXCL13, which mediates B-cell recruitment into androgen-deprived PC (8). CXCL13 also enhances LT production by B cells (24), and its expression in human PC correlates with clinical severity even better than prostate-specific antigen, the conventional PC biomarker (25). CXCL13 can be produced by osteoblasts and bone marrow mesenchymal cells, and this was proposed to mediate recruitment of PC cells that express the CXCL13 receptor, C-X-C motif receptor 5, into the bone microenvironment (26). We now show that myofibroblasts, which are activated by hypoxia and autocrine TGF-β signaling on androgen ablation, are responsible for B-cell recruitment into the tumor remnant, leading to accelerated malignant progression and CRPC development. We describe three different approaches to the targeting of myofibroblasts, all of which delay or prevent CRPC development.

Results

Tumor Myofibroblasts Express CXCL13. Using Myc-CaP allografts of androgen-dependent mouse PC (27), we examined how androgen ablation causes induction of CXCL13, which is needed for the recruitment of B cells into tumor remnants and accelerated CRPC evolution (8). Myc-CaP cells were inoculated s.c. into 6-wk-old FVB/N males, and when tumors reached 1,000 mm³ in size, the mice were castrated to deprive the tumors of androgens. After castration, we found many myofibroblasts positive for SMA within the tumor remnants and highly elevated expression of CXCL13 mRNA (Fig. 1*A*). To identify which cells express CXCL13, we isolated different cell types from androgen-deprived tumors and subjected them to PCR analysis. The mRNAs for CXCL13 and fibroblast activation protein (FAP), an enzyme that is expressed in mesenchymal stem cells and stromal fibroblasts (28) and that can serve as another myofibroblast marker (29), were detected only in the fibroblast fraction, not in the epithelial fraction prepared 1 wk after castration (Fig. 1*B*). The tumoral CD11b⁺ and CD11c⁺ fractions were also negative for CXCL13 and FAP mRNA (Fig. S1*A*). Flow cytometry showed that CD45⁻, 38-kDa glycoprotein (GP38)-positive (another myofibroblast marker), CXCL13⁺, and CXCL13⁺SMA⁺ cells were increased within the tumor remnants 1 wk after castration (Fig. 1*C*).

To deplete FAP⁺ cells in the androgen-deprived tumor stroma, we orally administered a DNA vaccine encoding FAP that is delivered to secondary lymphoid tissues by a noninfectious, attenuated, live *Salmonella typhimurium* vector (TOPO) (30). This strategy induces a strong cytotoxic T-cell response that results in specific killing of myofibroblasts within the tumor stroma of mammary cancer (30). Ablation of FAP-expressing cells with this vaccine also resulted in the disappearance of myofibroblasts that express CXCL13 in the stroma of androgen-deprived Myc-CaP tumors (Fig. 1*D*). Importantly, immunoablation of FAP⁺ cells was as effective as the genetic or antibody-mediated ablation of
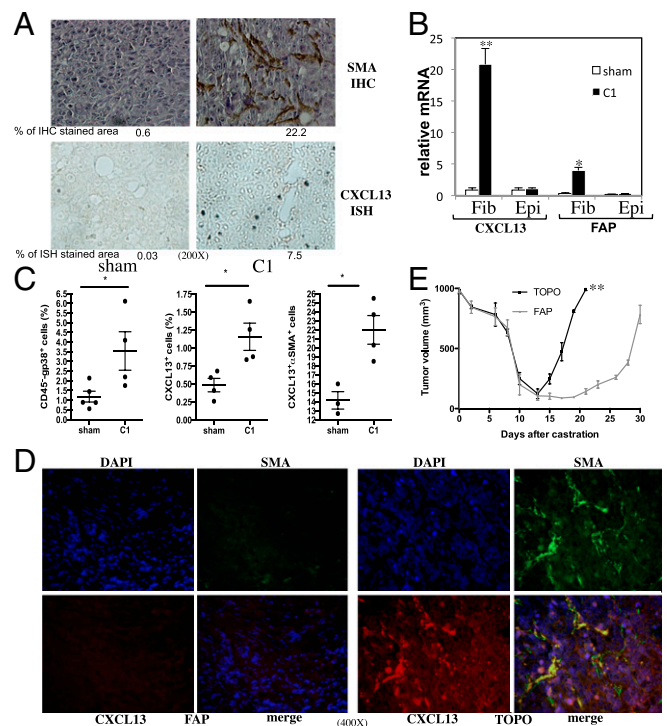

Fig. 1. Androgen ablation induces CXCL13 in myofibroblasts. (*A*) Six-week-old FVB/N males (*n* = 10) were s.c. inoculated with Myc-CaP cells. When the tumors reached 1,000 mm³, mice were castrated or sham operated. Tumors were examined 1 wk later for SMA by immunohistochemistry (IHC) and CXCL13 mRNA by in situ hybridization (ISH). (Magnification: 200×.) Areas occupied by positive cells were determined by image analysis (*n* = 2). (*B*) FVB/N mice (*n* = 10 per group) bearing Myc-CaP tumors were castrated or sham operated and killed 1 wk later. Tumors were removed and digested, and the fibroblast (Fib) and epithelial (Epi) cell fractions were isolated, total RNA was extracted, and CXCL13 and FAP mRNAs were quantitated by quantitative PCR (Q-PCR) and normalized to cyclophilin A mRNA. Results are averages ± SD. (*C*) FVB/N mice (*n* = 9) bearing Myc-CaP tumors were castrated or sham operated, and tumors were collected 1 wk later. CD45, CXCL13, SMA, and GP38 expression was analyzed by flow cytometry. (*D*) Six-week-old male FVB/N mice (*n* = 10 per group) were vaccinated three times with 10⁸ cfu of TOPO or FAP vaccines every 5 d. Myc-CaP tumors were established as described earlier. Three days before castration, the mice were vaccinated again. One week after castration, tumors were collected, paraffin-embedded, sectioned, counterstained with DAPI, and analyzed by immunofluorescence (IF) for SMA and CXCL13 expression. (Magnification: 400×.) (*E*) FVB/N males (*n* = 10 per group) were vaccinated and Myc-CaP tumors were established as described earlier. Tumor volume was measured every 2–3 d after castration. Results are expressed as means ± SEM.

B cells (8) in retarding the evolution of CRPC after castration of mice bearing Myc-CaP tumors (Fig. 1*E*). Ablation of FAP-expressing cells also led to a marked reduction in the infiltration of T and B lymphocytes and dendritic cells into the tumor remnants after castration but had little effect on the infiltration of F4/80⁺ macrophages (Figs. S1*B* and S2). FAP vaccination reduced expression of several other chemokines in addition to CXCL13, but expression of CCL19 and CCL20 increased (Fig. S1*C*). Consistent with its ability to block B-cell infiltration into androgen-deprived tumors, the FAP vaccine prevented IKKα nuclear translocation in cancer cells (Fig. S1*D* and *E*). These results suggest that CXCL13 is mainly expressed by activated myofibroblasts in the tumor microenvironment after castration. Interestingly, most FAP⁺ cells coexpressed SMA, but some SMA⁺ cells were FAP-negative (Fig. S3*A*). This is in line with recent findings that describe a heterogeneous population of stromal fibroblasts in which

FAP^{+} cells share markers with mesenchymal stem cells and the SMA[+] subset resembles fibrocytes (28). Curiously, when androgen-deprived Myc-CaP tumors grow back to 1,000 mm[3] in size, SMA^{+} cells are still absent, ruling out the possibility that repopulation with SMA^{+} cells (Fig. S3B) accounts for tumor recurrence in this system.

Role of TGF-β Signaling in CXCL13 Induction. Androgen ablation increased expression of TGF-β1, TGF-β2, and TGF-β3 in tumor remnants, reaching a peak 4 d after castration (Fig. 2A). Because TGF-β is known to be involved in fibroblast activation (21), we blocked TGF-β signaling with a specific inhibitor of TGF-β type 1 receptor (TGF-βR1)/activin receptor-like kinases (ALK4, ALK5, or ALK7), SB-431542 (31). Inhibition of TGF-βR1 signaling prevented activation of myofibroblasts (Fig. S4A), as well as nuclear translocation of small mothers against decapentaplegic (SMAD)2/3, infiltration of B cells, induction of CXCL13-expressing myofibroblasts, and nuclear translocation of IKKα (Fig. 2 B–E). SB-431542 treatment also delayed CRPC regrowth (Fig. 2F), reduced expression of several chemokine mRNAs other than CXCL13 within the tumors, and inhibited recruitment of B and T lymphocytes, as well as natural killer cells, dendritic cells, and macrophages and expression of TGF-β signaling targets such as forkhead box P3 (32) and SMAD7 (33) (Figs. S4 B–D and S5). After castration, FAP expression peaked at day 4, whereas CXCL13 induction and B-cell recruitment started peaking at day 6; all of these events were inhibited by SB-431542, which also inhibited castration-induced myofibroblast activation in the normal prostate (Fig. S4 D and E).

The main source of TGF-β in androgen-deprived Myc-CaP tumors is also the fibroblast fraction, rather than the epithelial or the myeloid CD11b^{+} or CD11c^{+} populations (Fig. S6 A and B). After castration, there is also an increase in the abundance of mRNAs coding for GP38 (34), connective tissue growth factor (CTGF), and insulin-like growth factor 1 (IGF1), particularly at 4 d after castration for GP38 and CTGF mRNAs (Fig. S7A). Ablation of FAP^{+} cells with the FAP vaccine significantly reduced the castration-elicited induction of IGF1, CTGF, and TGF-β family members (Fig. S6C), confirming that these growth factors are expressed by FAP[+] myofibroblasts. Previous studies have shown that CTGF can potentiate TGF-β signaling (21). Stimulation of inactive fibroblasts isolated from Myc-CaP tumors of sham-operated mice with CTGF plus TGF-β1 induced FAP, SMA, and CXCL13 mRNAs, but treatment of these cells with either TGF-β1 or CTGF alone was ineffective (Fig. 3A). Fibroblasts isolated from Myc-CaP tumors 1 wk after castration showed the expected elevated expression of FAP and SMA, but CXCL13 expression was not retained after cell isolation (Fig. 3A). Nonetheless, in these cells, TGF-β1 alone was sufficient for CXCL13 mRNA induction. FAP and SMA, but not CXCL13, mRNAs were also induced in fibroblasts from sham-operated mice on treatment with either IGF1 alone or IGF1 plus CTGF, but not by CTGF alone (Fig. S7B). In fibroblasts from androgen-deprived tumors, which already expressed FAP and SMA mRNAs, CXCL13 mRNA expression was induced by IGF1 (Fig. S7B). However, IGF1 is unlikely to have a critical role in CXCL13 induction in androgen-deprived tumors because its expression is increased only at 7 d after castration (Fig. S7A), whereas myofibroblasts are already activated after 4 d and CXCL13 is expressed at maximal levels at 6 d postcastration (Fig. S4E).

TGF-β Expression Is Induced by Hypoxia. Because castration results in injury to androgen-dependent tissues, and after injury the ensuing hypoxia is thought to be one of the main factors that triggers wound healing (35), a process that entails myofibroblast activation, we decided to study the role of hypoxia in fibroblast activation and CXCL13 induction. Culturing of inactive fibroblasts isolated from Myc-CaP tumors of noncastrated mice under hypoxic conditions converted the cells into myofibroblasts, as
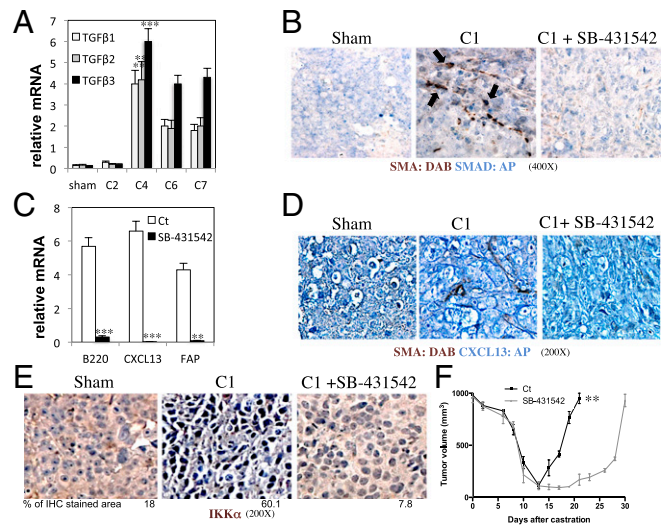

Fig. 2. Castration-induced myofibroblast activation depends on TGF-β signaling. (A) Myc-CaP tumors (n = 10) were established as in Fig. 1A and were collected after sham operation (7 d) or at the indicated days after castration (C2, C4, C6, C7 refer to 2, 4, 6, and 7 d postcastration). (B–E) FVB/N mice bearing Myc-CaP tumors were castrated. Starting 1 d before castration, mice (n = 10 per group) were injected daily with vehicle or SB-431542 (0.2 mg/mouse; 10 mg/kg), a TGF-βR1 inhibitor. Tumors were collected 1 wk after castration and analyzed by IHC for SMA and nuclear SMAD2/3, SMA and CXCL13, and IKKα or subjected to RNA extraction and Q-PCR analysis of the indicated mRNAs normalized to the amount of cyclophilin A mRNA (C results are averages ± SD). (Magnification: B, 400×; D, 200×; E, 200×.) The area occupied by nuclear IKKα-expressing cells was determined as defined earlier. (F) Tumors were established and mice were treated with SB-431542 or vehicle, as described earlier. Tumor volume was measured every 2–3 d. Results are expressed as means ± SEM. P values >0.05 were considered nonsignificant, 0.01–0.05 was considered significant (*), 0.001–0.01 was considered very significant (**), and <0.001 was considered highly significant (***).

judged by FAP and SMA expression, and led to the induction of CXCL13, CTGF, IGF1, and TGF-β mRNAs (Fig. 3B). Hypoxia also led to the induction of CTGF, IGF1, TGF-β, and CXCL13 mRNAs in fibroblasts of Myc-CaP tumors removed from castrated mice, although these fibroblasts were already activated, as indicated by FAP and SMA expression (Fig. 3B).

Importantly, 2 d after surgical castration, hypoxic areas revealed by staining with Hypoxyprobe (Hypoxyprobe, Inc) appeared within the tumors, along with nuclear translocation of hypoxia-inducible factor 1α (HIF-1α) in both cancer cells and stromal cells (Fig. 3C and Figs. S8 and S9). The hypoxic response may be caused by disruption of tumoral blood vessels, which is seen at 2 d after castration, based on staining with a CD34 antibody (Fig. S10A). Curiously, CD34^{+} cells reappear 8 d after castration, a point that precedes tumor regrowth and follows infiltration of androgen-deprived tumors with immune and inflammatory cells (8). Notably, the CD34^{+} cells that reappear at 8 d after castration are not as tightly organized as the CD34^{+} cells that reside within the tumors before castration (Fig. S10A). Deletion of HIF-1α in fibroblasts isolated from Hif-1α[F/F] mice using ectopic Cre recombinase (36) prevented their hypoxia-induced conversion into myofibroblasts (Fig. S10B). Induction of CTGF, IGF1, and TGF-β mRNAs under hypoxic conditions was also dependent on HIF-1α (Fig. S10C). CTGF, TGF-β1, TGF-β2, and TGF-β3 expression were previously described as being controlled by HIF-1α (37–40).

Phosphodiesterase 5 Inhibition Delays CRPC by Preventing Myofibroblast Activation. Phosphodiesterase 5 (PDE5) belongs to the phosphodiesterase superfamily of enzymes that catalyze hydrolysis of the cyclic nucleotides cAMP and cGMP to their 5′-nucleoside
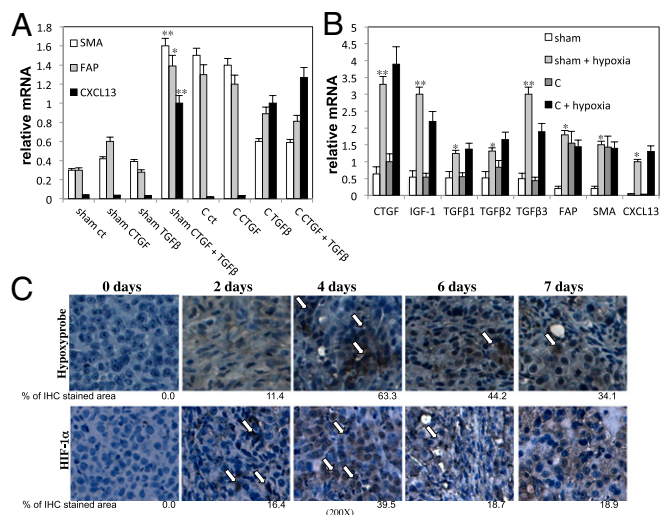
Fig. 3. Hypoxia caused by androgen ablation induces TGF-β, CTGF, and IGF1 expression. (*A*) Fibroblasts were purified from Myc-CaP tumors 1 wk after sham operation or castration (C) (*n* = 10 per group), plated, and stimulated for 24 h with TGF-β1 (10 ng/mL), CTGF (50 ng/mL), or TGF-β1 plus CTGF. RNA was isolated, and expression of the indicated genes was analyzed as described earlier. Results are averages ± SD. (*B*) Fibroblasts were isolated from Myc-CaP tumors 1 wk after castration (C) or sham operation and incubated either in a standard incubator or a hypoxic chamber (1% O₂) for 24 h. Total RNA was isolated, and the indicated mRNAs were quantitated. Results are averages ± SD (*C*) FVB/N mice bearing Myc-CaP tumors were castrated, and tumors were collected at indicated times after castration. For hypoxia analysis, mice were i.p. injected 90 min before sacrifice with 60 mg/kg of pimonidazole hydrochloride (Hypoxyprobe-1). Tumors were removed, fixed, paraffin-embedded, sectioned, and subjected to IHC with Hypoxyprobe or HIF-1α antibodies. (Magnification: 200×.) The areas occupied by positive cells were determined as described earlier. Arrows indicate hypoxic areas and cells with nuclear HIF-1α.

monophosphates (41). Two specific PDE5 inhibitors, tadalafil and vardenafil, attenuate TGF-β1–induced myofibroblast activation in the prostate (42, 43). We found that treatment of mice with another PDE5 inhibitor, sildenafil, significantly delayed CRPC emergence in castrated Myc-CaP tumor-bearing mice (Fig. 4*A*). IHC analysis 1 wk postcastration revealed that the number of SMA⁺ activated myofibroblasts in the tumor remnants was significantly reduced in mice treated with sildenafil versus controls (Fig. 4*B*). Exposure of fibroblasts isolated from sham-operated tumors to hypoxia for 24 h in presence of a generic PDE inhibitor, pentoxifylline (44), or sildenafil blocked myofibroblast activation, as judged by SMA mRNA expression, and also reduced CXCL13 and TGF-β mRNA abundance (Fig. 4*C*).

Myofibroblast Activation in Transgenic Adenocarcinoma of the Mouse Prostate Tumors and Normal Prostate. Castration also led to induction of inflammatory cytokines, including LTα, LTβ, IL-6, receptor activator of nuclear factor kappa-B ligand, and IL-17b, as well as CXCL13, TGF-β, immune infiltration, and myofibroblast activation in the normal prostate, an androgen-dependent organ (Fig. 5 *A* and *B*). Similar findings were obtained in the spontaneous PC transgenic adenocarcinoma of the mouse prostate (TRAMP) model (45), which develops metastatic tumors with neuroendocrine differentiation (46). In particular, we observed induction of CXCL13, LTα, LTβ, and TGF-β mRNAs; myofibroblast activation; HIF-1α nuclear translocation; and B-cell infiltration at 7 wk after the castration of TRAMP mice (Fig. 5 *C* and *D* and Fig. S11 *A* and *B*). Interestingly, the induction of CXCL13, LTα, LTβ, and TGF-β mRNAs is transient, and the levels go back to normal at 12 wk. The nature of the transient induction was

previously explained (8). Androgen ablation induces injury in the tumor remnants, which causes a transient increase of inflammatory cytokines and cells. This inflammatory response ceases once the tumor begins to grow back exponentially. Similar to the Myc-CaP model, most SMA⁺ cells were also FAP-positive (Fig. S11*C*). The effect of myofibroblast ablation with the FAP vaccine on TRAMP mice was even more striking than in the Myc-CaP model; almost no tumor tissue remained at 7 wk after castration in TRAMP mice that were vaccinated with the FAP vector (Fig. 5*E*). In addition to almost complete myofibroblast ablation (Fig. S11 *D* and *E*), FAP-vaccinated TRAMP mice exhibited more apoptotic cell death within prostate tumors after castration relative to castrated mice that received the control TOPO vaccine (Fig. S11*F*).

Myofibroblast Activation and CXCL13 Expression in Human PC. We also examined whether the human PC microenvironment contains fibroblasts that express CXCL13 and myofibroblast markers. Using specimens of normal and cancerous prostate tissue, we found substantially higher expression of CXCL13 and nuclear HIF-1α in malignant prostate tissue compared with normal tissue or benign prostatic hyperplasia, although the latter specimens did contain SMA⁺ and FAP⁺ myofibroblasts (Fig. 6*A* and Fig. S12 *A* and *B*). We also found that CXCL13 and SMA were colocalized in malignant prostate tissue (Fig. 6*B*) and that B cells in malignant tissues were located next to CXCL13-expressing cells (Fig. 6*C*).

Discussion

CAFs exert many important functions during tumor development and progression (12), including organization and shaping of the tumor microenvironment (47). Here we show that activated CAFs that express myofibroblast markers are a critical source of CXCL13, the major B-cell chemoattractant (48), in androgen-deprived mouse prostate tumors and human PC. Importantly, CXCL13 induction and myofibroblast activation are not unique to androgen-deprived s.c. transplanted PC allografts but were also observed on castration in the spontaneous PC TRAMP model and even in the normal prostate, which also contains cells that die on androgen deprivation, thereby leading to tissue injury and hypoxia. By uncovering myofibroblasts as the critical source of CXCL13 in androgen-deprived PC, we
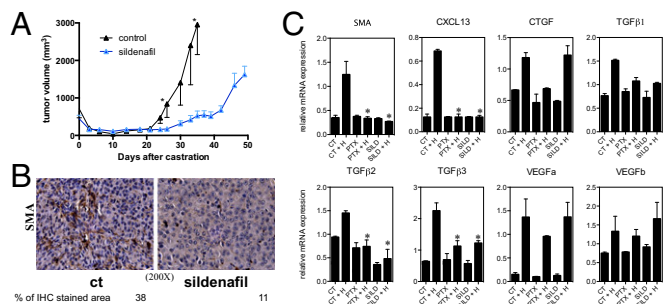

Fig. 4. PDE5 inhibition attenuates CRPC by interfering with myofibroblast activation. (*A* and *B*) Tumors were established in 6-wk-old FVB/N males (*n* = 10), as described earlier. Sildenafil was either added or not to the drinking water (0.7 g/L). (*A*) Tumor volume was measured every 2–3 d. Results are averages ± SEM. (*B*) Tumors were collected 1 wk after castration and analyzed for SMA by IHC. The areas occupied by SMA⁺ cells were determined as described earlier (*n* = 2). (*C*) Tumor-associated fibroblasts were purified from mice bearing Myc-CaP tumors and incubated in either a standard incubator or an hypoxic chamber (1% O₂) for 24 h in the absence or presence of indicated inhibitors. CT, control; H, hypoxia; PTX, pentoxyfidine; SILD, sildenafil. Expression of the indicated mRNAs was analyzed by Q-PCR as described earlier (*n* = 5). Results are averages ± SD.
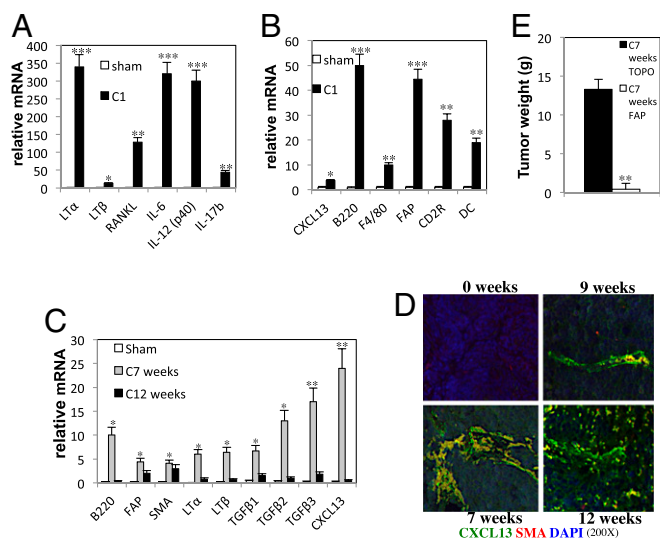
Fig. 5. Myofibroblasts are required for CXCL13 expression and control TRAMP tumor malignant progression. (*A* and *B*) Six-week-old FVB/N males (*n* = 10 per group) were castrated or sham operated, and their prostates were collected 1 wk after surgery. The indicated inflammatory cytokines and chemokines and cell marker mRNAs were quantitated by Q-PCR, as described earlier. Results are averages ± SD. (*C* and *D*) Twelve-week-old TRAMP males (*n* = 10) were castrated or sham operated, and their tumors were collected at the indicated times after castration. Expression of indicated mRNAs was quantified by Q-PCR, as described earlier. Results are averages ± SD (*C*). Tumors were fixed, paraffin embedded, sectioned, counterstained with DAPI, and analyzed for SMA and CXCL13 by IF (*D*). (Magnification: 200×.) (*E*) Six-week-old TRAMP males (*n* = 10 per group) were vaccinated three times with 10^8 cfu of TOPO or FAP vaccines every 5 d, followed by a booster shot every 30 d. Mice were castrated when 12 wk old, and tumor weight was measured after 7 wk. Results are averages ± SD.

identified an important function of these cells that has not been previously described: their ability to undergo rapid activation in response to tumor hypoxia and produce a number of chemokines. Although hypoxia is a normal feature of tumor development that is usually seen in the core of rapidly growing tumors (49), we show that androgen ablation leads to a strong and rapid increase in tumor hypoxia, presumably because of blood vessel collapse/destruction within androgen-dependent tumors and tissues. Importantly, myofibroblasts derived from proliferating fibroblasts (20, 21) are distinct from senescent CAFs (50), which are induced to produce proinflammatory cytokines, chemokines, and growth factors in prostate tumors subjected to genotoxic stress (23). Production of cytokines and growth factors by CAFs that have undergone senescence on genotoxic stress is mediated through the DNA damage response, which leads to activation of NF-κB (23). In our system, however, the critical source of CXCL13 is myofibroblasts, rather than senescent fibroblasts. Consistent with the different mechanisms that lead to cytokine and chemokine secretion by CAFs after genotoxic therapy or androgen ablation, it is not unexpected that each condition elaborates a distinct cytokine/chemokine profile, with CXCL13 induction being stronger after androgen ablation than after genotoxic stress. Nonetheless, the destruction of tumor blood vessels by radiation and chemotherapy (51) raises the possibility that both mechanisms may contribute to PC recurrence after therapy, especially when chemotherapy or radiotherapy are used in combination with androgen receptor antagonists.

Using cultured CAFs from prostate tumors, we show that one of the most effective ways to convert these cells into myofibroblasts and induce CXCL13 expression is to subject them to

hypoxia. This results in the activation of HIF-1, the HIF-1α subunit of which is stabilized under hypoxic conditions and modulates transcription by interacting with coactivators such as p300/CBP (52). Notably, hypoxia leads to autocrine production of TGF-β family members and CTGF, growth factors that, if applied together to cultured CAFs, can also lead to myofibroblast activation and CXCL13 induction. Thus, hypoxia can create a self-amplifying, TGF-βR1-dependent, autoregulatory loop that results in potent CXCL13 induction. Importantly, HIF-1α activation, TGF-β, and CTGF induction and SMAD2/3 activation have all been observed in vivo in response to androgen ablation. Furthermore, the TGF-β1, TGF-β2, TGF-β3, and CTGF genes were described as HIF-1α target genes (37–40). We postulate that the sequence of events that leads to myofibroblast activation in androgen-deprived prostates and PC includes hypoxia, HIF-1 activation, induction of TGF-β and CTGF, and activation of autocrine SMAD signaling. Using the TGF-βR1/ALK5 inhibitor SB-431542, we show that inhibition of SMAD activation prevents myofibroblast activation, CXCL13 induction, and B-cell recruitment and slows down CRPC development. At this point, however, it is not clear whether CXCL13 is a direct SMAD target or whether it is regulated through other transcription factors that are activated when fibroblasts become myofibroblasts.

PDE5 inhibitors attenuate TGF-β1-induced fibroblast-to-myofibroblast *trans*-differentiation in the prostate and are used in the treatment of benign prostatic hyperplasia (42, 43). We took advantage of this interesting finding and tested the ability of the PDE5 inhibitor sildenafil to inhibit castration-induced myofibroblast activation and CXCL13 induction. PDE5 inhibition was as effective as TGF-βR1 inhibition or immune-mediated depletion of myofibroblasts in blocking CXCL13 induction and B-cell recruitment and in delaying CRPC emergence. Altogether, these results raise the prospect of myofibroblast targeting in PC therapy. Because senescent fibroblasts and myofibroblasts affect PC progression and resistance to therapy through different mechanisms, we suggest that both CAF populations need to be targeted to improve the effectiveness of existing PC therapy. However, as far as myofibroblast targeting is concerned, it is probably advantageous to target these cells through inhibition of PDE5 activity or TGF-βR1 signaling, rather than eliminate these cells through FSP vaccination. Importantly, myofibroblasts play an essential role in wound healing, being responsible for collagen production, ECM deposition, and formation of scar tissue (53). In addition, FAP ablation experiments have demonstrated that FAP+ cells have an important tissue-protective function because they either suppress the production of TNF and IFN-γ or attenuate cellular responses to these cytokines (28). FAP+ myofibroblasts
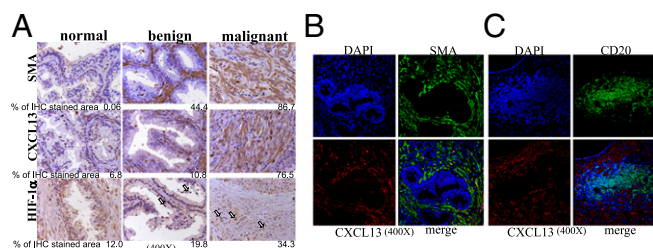

Fig. 6. SMA, CXCL13, and HIF-1α are highly expressed in malignant human PC tissue. (*A–C*) Paraffin-embedded human prostate tissues [normal (*n* = 5), benign hyperplasia (*n* = 4), and malignant (*n* = 10)] were sectioned and analyzed for SMA, CXCL13, and HIF-1α by IHC. Shown are typical examples of each case. (*A*) The areas occupied by positive cells were calculated as described earlier. (Magnification: 400×.) The human prostate samples were also stained for SMA and CXCL13 (*B*) or CD20 and CXCL13 (*C*) and analyzed by IF. (Magnification: 400×.)

are also closely related to lymphoid tissue stromal cells, which are needed for proper immune functions (54). An even better approach to CAF targeting would be to target CAF-produced factors, such as CXCL13 (8) and WNT16B (23), which mediate some of the CAF-generated effects on tumor recurrence and resistance to therapy.

It is notable that a PDE5 inhibitor, tadalafil, is already approved for benign prostatic hyperplasia treatment (55). Therefore, its repurposing in PC treatment to prevent malignant progression in tumors subjected to androgen ablation or chemotherapy should be relatively straightforward. Indeed, the adverse effects of PDE5 inhibitors are almost negligible compared with more aggressive approaches, such as chemotherapy and radiotherapy.

Materials and Methods

Detailed methods are available in *SI Materials and Methods*. Briefly, mice were handled according to Institutional and National Institutes of Health guidelines. Human material was obtained from the Cooperative Human Tissue Network, along with pathology reports. Histology and gene expression were analyzed as described (8).

1. Jemal A, et al. (2011) Global cancer statistics. *CA Cancer J Clin* 61(2):69–90.
2. Hirano D, Hasegawa R, Satoh K, et al. (Apri 15, 2014) Prospective study on the relationship between clinical efficacy of secondary hormone therapy with flutamide and neuroendocrine differentiation in patients with relapsed prostate cancer after first line hormone therapy. *Scand J Urol*, doi:10.3109/21681805.2014.905633.
3. Beltran H, et al. (2012) Challenges in recognizing treatment-related neuroendocrine prostate cancer. *J Clin Oncol* 30(36):e386–e389.
4. Beltran H, Rickman DS, Park K, et al. (2011) Molecular characterization of neuroendocrine prostate cancer and identification of new drug targets. *Cancer Discov* 1(6):487–495.
5. Terry S, Beltran H (2014) The many faces of neuroendocrine differentiation in prostate cancer progression. *Front Oncol* 4:60.
6. Gueron G, De Siervi A, Vazquez E (2012) Advanced prostate cancer: Reinforcing the strings between inflammation and the metastatic behavior. *Prostate Cancer Prostatic Dis* 15(3):213–221.
7. So A, Gleave M, Hurtado-Col A, Nelson C (2005) Mechanisms of the development of androgen independence in prostate cancer. *World J Urol* 23(1):1–9.
8. Ammirante M, Luo JL, Grivennikov S, Nedospasov S, Karin M (2010) B-cell-derived lymphotoxin promotes castration-resistant prostate cancer. *Nature* 464(7286):302–305.
9. Woo JR, et al. (2014) Tumor infiltrating B-cells are increased in prostate cancer tissue. *J Transl Med* 12:30.
10. Luo JL, et al. (2007) Nuclear cytokine-activated IKKalpha controls prostate cancer metastasis by repressing Maspin. *Nature* 446(7136):690–694.
11. Bhowmick NA, Neilson EG, Moses HL (2004) Stromal fibroblasts in cancer initiation and progression. *Nature* 432(7015):332–337.
12. Hanahan D, Coussens LM (2012) Accessories to the crime: Functions of cells recruited to the tumor microenvironment. *Cancer Cell* 21(3):309–322.
13. Kalluri R, Zeisberg M (2006) Fibroblasts in cancer. *Nat Rev Cancer* 6(5):392–401.
14. Shimoda M, Mellody KT, Orimo A (2010) Carcinoma-associated fibroblasts are a rate-limiting determinant for tumour progression. *Semin Cell Dev Biol* 21(1):19–25.
15. Dirat B, et al. (2011) Cancer-associated adipocytes exhibit an activated phenotype and contribute to breast cancer invasion. *Cancer Res* 71(7):2455–2465.
16. Erez N, Truitt M, Olson P, Arron ST, Hanahan D (2010) Cancer-Associated Fibroblasts Are Activated in Incipient Neoplasia to Orchestrate Tumor-Promoting Inflammation in an NF-kappaB-Dependent Manner. *Cancer Cell* 17(2):135–147.
17. Cirri P, Chiarugi P (2011) Cancer associated fibroblasts: The dark side of the coin. *Am J Cancer Res* 1(4):482–497.
18. Räsänen K, Vaheri A (2010) Activation of fibroblasts in cancer stroma. *Exp Cell Res* 316(17):2713–2722.
19. Lee SB, Kalluri R (2010) Mechanistic connection between inflammation and fibrosis. *Kidney Int Suppl* (119):S22–S26.
20. LeBleu VS, et al. (2013) Origin and function of myofibroblasts in kidney fibrosis. *Nat Med* 19(8):1047–1053.
21. Grotendorst GR, Rahmanie H, Duncan MR (2004) Combinatorial signaling pathways determine fibroblast proliferation and myofibroblast differentiation. *FASEB J* 18(3):469–479.
22. Velarde MC, Demaria M, Campisi J (2013) Senescent cells and their secretory phenotype as targets for cancer therapy. *Interdiscip Top Gerontol* 38:17–27.
23. Sun Y, et al. (2012) Treatment-induced damage to the tumor microenvironment promotes prostate cancer therapy resistance through WNT16B. *Nat Med* 18(9):1359–1368.
24. Ansel KM, et al. (2000) A chemokine-driven positive feedback loop organizes lymphoid follicles. *Nature* 406(6793):309–314.
25. Singh S, et al. (2009) Serum CXCL13 positively correlates with prostatic disease, prostate-specific antigen and mediates prostate cancer cell invasion, integrin clustering and cell adhesion. *Cancer Lett* 283(1):29–35.
26. Singh S, Singh R, Singh UP, et al. (2009) Clinical and biological significance of CXCR5 expressed by prostate cancer specimens and cell lines. *Int J Cancer* 125(10):2288–2295.
27. Watson PA, et al. (2005) Context-dependent hormone-refractory progression revealed through characterization of a novel murine prostate cancer cell line. *Cancer Res* 65(24):11565–11571.
28. Kraman M, et al. (2010) Suppression of antitumor immunity by stromal cells expressing fibroblast activation protein-alpha. *Science* 330(6005):827–830.
29. Chen H, Yang WW, Wen QT, Xu L, Chen M (2009) TGF-beta induces fibroblast activation protein expression; fibroblast activation protein expression increases the proliferation, adhesion, and migration of HO-8910PM [corrected]. *Exp Mol Pathol* 87(3):189–194.
30. Loeffler M, Krüger JA, Niethammer AG, Reisfeld RA (2006) Targeting tumor-associated fibroblasts improves cancer chemotherapy by increasing intratumoral drug uptake. *J Clin Invest* 116(7):1955–1962.
31. Inman GJ, et al. (2002) SB-431542 is a potent and specific inhibitor of transforming growth factor-beta superfamily type I activin receptor-like kinase (ALK) receptors ALK4, ALK5, and ALK7. *Mol Pharmacol* 62(1):65–74.
32. Tone Y, et al. (2008) Smad3 and NFAT cooperate to induce Foxp3 expression through its enhancer. *Nat Immunol* 9(2):194–202.
33. Stopa M, et al. (2000) Participation of Smad2, Smad3, and Smad4 in transforming growth factor beta (TGF-beta)-induced activation of Smad7. THE TGF-beta response element of the promoter requires functional Smad binding element and E-box sequences for transcriptional regulation. *J Biol Chem* 275(38):29308–29317.
34. Roozendaal R, Mebius RE (2011) Stromal cell-immune cell interactions. *Annu Rev Immunol* 29:23–43.
35. Guo S, Dipietro LA (2010) Factors affecting wound healing. *J Dent Res* 89(3):219–229.
36. Ryan HE, Lo J, Johnson RS (1998) HIF-1 alpha is required for solid tumor formation and embryonic vascularization. *EMBO J* 17(11):3005–3015.
37. Higgins DF, et al. (2004) Hypoxic induction of Ctgf is directly mediated by Hif-1. *Am J Physiol Renal Physiol* 287(6):F1223–F1232.
38. Zhang H, et al. (2003) Cellular response to hypoxia involves signaling via Smad proteins. *Blood* 101(6):2253–2260.
39. Schäffer L, et al. (2003) Oxygen-regulated expression of TGF-beta 3, a growth factor involved in trophoblast differentiation. *Placenta* 24(10):941–950.
40. Basu RK, et al. (2011) Interdependence of HIF-1α and TGF-β/Smad3 signaling in normoxic and hypoxic renal epithelial cell collagen expression. *Am J Physiol Renal Physiol* 300(4):F898–F905.
41. Rosen RC, McKenna KE (2002) PDE-5 inhibition and sexual response: Pharmacological mechanisms and clinical outcomes. *Annu Rev Sex Res* 13:36–88.
42. Zenzmaier C, et al. (2010) Attenuated proliferation and trans-differentiation of prostatic stromal cells indicate suitability of phosphodiesterase type 5 inhibitors for prevention and treatment of benign prostatic hyperplasia. *Endocrinology* 151(8):3975–3984.
43. Zenzmaier C, et al. (2012) Phosphodiesterase type 5 inhibition reverts prostate fibroblast-to-myofibroblast trans-differentiation. *Endocrinology* 153(11):5546–5555.
44. Nandi JS, Nair KG, Deo S (1980) Inhibition cAMP-phosphodiesterase in the rat heart by pentoxifylline—a new xanthine derivative. *Adv Myocardiol* 1:359–365.
45. Greenberg NM, et al. (1995) Prostate cancer in a transgenic mouse. *Proc Natl Acad Sci USA* 92(8):3439–3443.
46. Qi J, et al. (2010) Siah2-dependent concerted activity of HIF and FoxA2 regulates formation of neuroendocrine phenotype and neuroendocrine prostate tumors. *Cancer Cell* 18(1):23–38.
47. Xing F, Saidou J, Watabe K (2010) Cancer associated fibroblasts (CAFs) in tumor microenvironment. *Front Biosci (Landmark Ed)* 15:166–179.
48. Legler DF, et al. (1998) B cell-attracting chemokine 1, a human CXC chemokine expressed in lymphoid tissues, selectively attracts B lymphocytes via BLR1/CXCR5. *J Exp Med* 187(4):655–660.
49. Rundqvist H, Johnson RS (2010) Hypoxia and metastasis in breast cancer. *Curr Top Microbiol Immunol* 345:121–139.
50. Dean JP, Nelson PS (2008) Profiling influences of senescent and aged fibroblasts on prostate carcinogenesis. *Br J Cancer* 98(2):245–249.
51. Paris F, et al. (2001) Endothelial apoptosis as the primary lesion initiating intestinal radiation damage in mice. *Science* 293(5528):293–297.
52. Weidemann A, Johnson RS (2008) Biology of HIF-1alpha. *Cell Death Differ* 15(4):621–627.
53. Li B, Wang JH (2011) Fibroblasts and myofibroblasts in wound healing: Force generation and measurement. *J Tissue Viability* 20(4):108–120.
54. Peduto L, et al. (2009) Inflammation recapitulates the ontogeny of lymphoid stromal cells. *J Immunol* 182(9):5789–5799.
55. Cantrell MA, Baye J, Vouri SM (2013) Tadalafil: A phosphodiesterase-5 inhibitor for benign prostatic hyperplasia. *Pharmacotherapy* 33(6):639–649.